# Molecular Brushes with Spontaneous Gradient by Atom Transfer Radical Polymerization

**Hyung-il Lee,[†] Krzysztof Matyjaszewski,*[,†] Sherryl Yu,[‡] and Sergei S. Sheiko[‡]**

*Center for Macromolecular Engineering, Department of Chemistry, Carnegie Mellon University, 4400 Fifth Avenue, Pittsburgh, Pennsylvania 15213, and Department of Chemistry, University of North Carolina at Chapel Hill, North Carolina 27599-3290*

*Received June 11, 2005; Revised Manuscript Received July 29, 2005*

ABSTRACT: Spontaneous gradient copolymers were synthesized by atom transfer radical polymerization (ATRP) of acrylates and methacrylates and were subsequently employed to prepare macroinitiators for the synthesis of molecular brushes. Simultaneous copolymerizations of methyl methacrylate (MMA) and 2-(trimethylsilyloxy)ethyl acrylate (HEA-TMS) with different monomer feed ratios were conducted, and the resulting poly(MMA-*grad*-HEA-TMS) copolymers were transformed to a macroinitiator, poly(MMA-*grad*-(2-(2-bromopropionyloxy)ethyl acrylate) (BPE)). Another monomer pair of 2-(trimethylsilyloxy)ethyl methacrylate (HEMA-TMS) and *n*-butyl acrylate (*n*-BA) was also used for a simultaneous copolymerization for comparison between these two systems. Brushes were synthesized from these macroinitiators by the "grafting from" method with *n*-BA. The gradient composition of the backbone was formed spontaneously due to the difference in the reactivity ratios of the two monomers. The reactivity ratios were determined by nonlinear least-squares calculations for both monomer pairs from conversion data obtained by gas chromatography. AFM images confirmed the gradient shape of brushes by resolving two different ends of brushes: densely grafted heads and loosely grafted tails.

## Introduction

Recently, considerable interest has been drawn to molecular bottle brushes.[1−4] The controlled structure of bottle brushes on molecular dimensions facilitates designing materials with preprogrammed activity. Depending on the nature of the backbone and side chains, the molecular brushes can potentially be applied to supersoft elastomers.

Gradient copolymers can be prepared either by simultaneous copolymerization or by feeding one monomer into the reaction mixture.[5,6] In the former case, the controlled/living copolymerization of monomers with different reactivity ratios causes a continuous change in monomer composition in the reaction mixture, which results in a continuous change of composition along each individual polymer chain. In the latter case, comonomers with similar reactivities could be used, but a change of composition in the reaction mixture is accomplished by a continuous addition of one comonomer.[5−10] Methacrylate/acrylate pairs[11] were chosen for this study due to the relatively large differences in the monomer reactivity ratios in free radical polymerization. By using controlled/living radical polymerization, one can copolymerize two monomers simultaneously with good control to obtain a copolymer with a gradient of composition along its length. A gradient structure within a single polymer chain cannot be accomplished in a conventional radical system where polymer chains are continuously initiated and terminated. In this case, chains prepared at low conversion will have composition different from those prepared at high conversion.

It was reported that single molecular bottle brushes undergo rod−globule conformational transitions under lateral compression of a molecular monolayer on water.[12] In the case of gradient brushes, the rod−globule transition occurs only at the end where the brush is densely grafted, leaving a molecule with a globular "head" and an extended "tail".[13] This anisotropic transition of the gradient brushes led to tadpole conformations under compression.

Molecular bottle brushes can be synthesized by three different methods: "grafting to",[14,15] "grafting through",[2,16−18] and "grafting from".[18−21] To achieve a high grafting density, grafting from via ATRP has proven particularly beneficial.[18,21−24] For a methacrylate-based backbone, this is accomplished by a three-step process: ATRP of 2-(trimethylsilyloxy)ethyl methacrylate (HEMA-TMS) followed by transformation of the precursor polymer into poly(2-(2-bromopropionyloxy)-ethyl methacrylate) (pBPEM) and then grafting various monomers from the pBPEM macroinitiator.[5,19,20]

The synthesis and visualization of gradient copolymer brushes prepared by the forced gradient method were previously reported by our group. In this paper we report the syntheses of gradient copolymer brushes prepared by spontaneous gradient formation along the backbone and subsequent visualization of the resulting brushes by atomic force microscopy (AFM). The two monomer pairs of MMA/HEA-TMS and HEMA-TMS/*n*-BA were used due to the inherent difference in reactivity between acrylates and methacrylates in free radical polymerization. To understand and control the gradient structure along the backbone, the reactivity ratios of the copolymerizations for both monomer pairs were estimated by nonlinear least-squares calculations.

## Experimental Section

**Materials.** All chemicals were purchased from Aldrich, Polysciences, and Acros and used as received unless otherwise stated. MMA, *n*-BA, 2-(trimethylsilyloxy)ethyl methacrylate (HEMA-TMS), and 2-(trimethylsilyloxy)ethyl acrylate (HEA-TMS) were distilled under vacuum prior to use.[25] 4,4′-Di-(5-nonyl)-2,2′-bipyridine (dNbpy) was prepared as previously

[†] Carnegie Mellon University.
[‡] University of North Carolina at Chapel Hill.
* Corresponding author. E-mail: km3b@andrew.cmu.edu.

10.1021/ma051231z CCC: $30.25 
Published on Web 09/07/2005

**Scheme 1. Synthetic Outline for the Gradient Copolymer, Macroinitiator, and Molecular Brush: (a) MMA/HEA-TMS System; (b) HEMA-TMS/*n*-BA System**

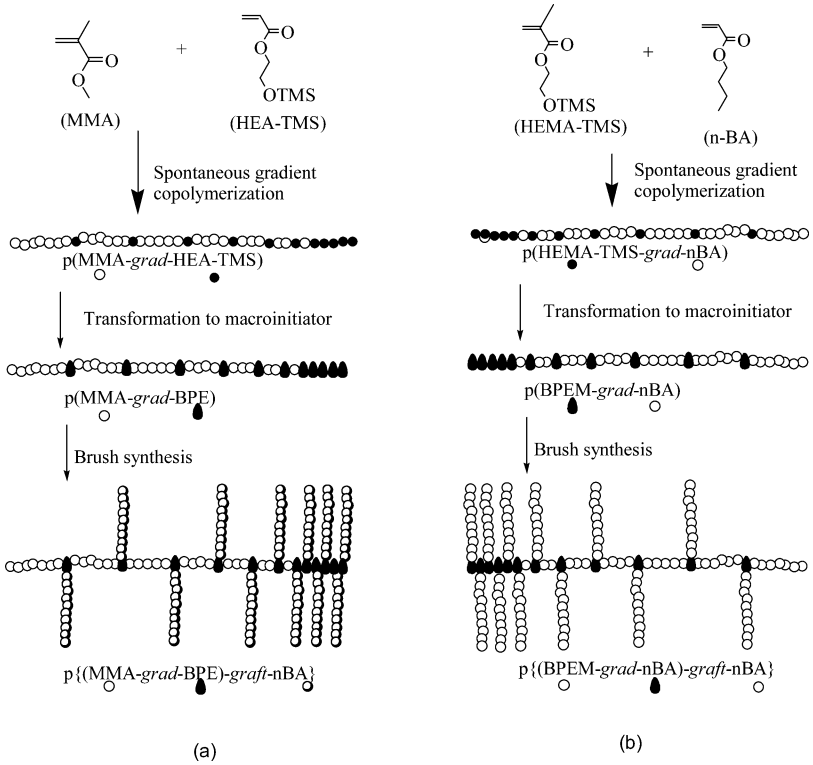


reported.[26] CuBr was purified as described previously,[10] and $CuBr_2$ was used as received.

**Analysis.** Monomer conversions were determined by gas chromatography (GC) from aliquots taken during the reaction with a Shimadzu GC 14A gas chromatograph equipped with a FID detector and a J & W Scientific 30 m DB608 column. The copolymer compositions of the macroinitiator backbones were determined by $^1$H NMR spectroscopy in $CDCl_3$ with a Bruker Avance DMX-300 spectrometer operating at 300 MHz. Absolute and apparent molecular weights were determined by GPC (Waters microstyragel columns (guard, $10^5$, $10^3$, and $10^2$ Å), THF eluent at 35 °C, flow rate = 1.00 mL/min). The detectors consisted of a differential refractometer (Waters 410) and a multiangle laser light scattering (MALLS) detector (Wyatt Technology DAWN EOS). Apparent molecular weights were determined with a calibration based on poly(methyl methacrylate) (PMMA) standards using WinGPC software from Polymer Standards Service.

**Synthesis.** p(MMA-*grad*-HEA-TMS) (**I**): initial feed ratio (MMA:HEA-TMS = 1:1). In a 10 mL round-bottom flask, ethyl 2-bromoisobutyrate (14.7 $\mu$L, 0.1 mmol) and anisole (3.6 mL, 50 vol %) were combined, and the solution was bubbled for 10 min at room temperature. In a 25 mL Schlenk flask, dNbpy (0.082 g, 0.2 mmol), MMA (3.0 g, 30 mmol), and HEA-TMS (5.6 g, 30 mmol) were added, and the resulting solution was degassed by three freeze−pump−thaw cycles. CuBr (0.014 g, 0.1 mmol) was added, and after stirring for 10 min, the Schlenk flask was placed in a thermostated oil bath at 85 °C. After 3 min, the initiator solution was transferred into the Schlenk flask, and an initial sample was taken. During polymerization, samples were removed periodically to determine molecular weight by GPC and conversion by GC. The reaction mixture was stirred for 8 h, exposed to air, diluted in $CH_3Cl$, and filtered through a neutral alumina column to remove the copper catalyst. Next, the solvent was removed, and the polymer was dried under vacuum to a constant weight. Monomer conversion was 97% of MMA and 75% of HEA-TMS (GC); $M_n$ (GPC) = 71 000; $M_w/M_n$ = 1.28.

p(MMA-*grad*-HEA-TMS) (**II**): initial feed ratio (MMA:HEA-TMS = 3:1). The procedure was the same as described reaction except that PMDETA was used as a ligand instead of dNbpy. Monomer conversion was 78% of MMA and 65% of HEA-TMS (GC); $M_n$ (GPC) = 51 000; $M_w/M_n$ = 1.21.

p(MMA-*grad*-BPE) (**IA**). The product of the p(MMA-*grad*-HEA-TMS) polymerization was placed in a 250 mL round-bottom flask (3.18 g, assuming 10.4 mmol of −OTMS groups). KF (0.604 g, 10.40 mmol) was added, the flask was sealed and flushed with $N_2$, and dry THF (125 mL) was added. A solution of tetrabutylammonium fluoride in THF (0.027 g, 0.03 mL, 0.10 mmol) was added dropwise to the flask, followed by the slow addition of 2-bromopropionyl bromide (3.37 g, 1.65 mL, 15.6 mmol) over the course of 15 min. The reaction mixture was stirred overnight at room temperature and precipitated into methanol/ice (80/20 v/v %). The separated precipitate was redissolved in $CHCl_3$ (100 mL) and filtered through a column of basic alumina, and the solvent was removed under vacuum. The isolated polymer was reprecipitated from THF once into MeOH and three times into hexanes and dried under vacuum at 25 °C for 24 h. $^1$H NMR (300 MHz, $CDCl_3$, $\delta$ in ppm): pBPE part: 4.52 (1H, quart, $J$ = 6.8 Hz, Br−C*H*−$CH_3$); 4.36 (2H, bs, −O−$CH_2$−C*H*$_2$−OCO−CH−Br); 4.15 (2H, bs, −O−C*H*$_2$−$CH_2$−O−CO−CH−Br); 1.82 (overlapped, d, $J$ = 6.8 Hz, Br−CH−C*H*$_3$); 2.3−1.73 (overlapped, m, C*H*$_2$−CH); 1.32−1.1 (overlapped, bs, $CH_2$−C*H*). pMMA part: 3.6 (3H, s, −O−C*H*$_3$); 2.15−1.37 (overlapped, m, $CH_3$−C−C*H*$_2$); 1.37−0.75 (overlapped, 3 × bs,C*H*$_3$−C−$CH_2$). $M_n$ (GPC) = 72 000; $M_w/M_n$ = 1.32, DP = 515.

p(MMA-*grad*-BPE) (**IIA**). The reaction procedure was the same as the above reaction (**IA**). $M_n$ (GPC) = 52 000; $M_w/M_n$ = 1.20. DP = 450.

p[(MMA-*grad*-(BPE-*graft*-*n*-BA)] (**IIA-1**). In a 100 mL Schlenk flask, p(MMA-*grad*-BPE) (0.2 g; 0.550 mmol initiating sites (from NMR spectroscopy measurements)), $CuBr_2$ (0.0028 g, 0.0126 mmol), and dNbpy (0.206 g, 0.51 mmol) were purged three times with nitrogen. Deoxygenated *n*-BA (25.92 g, 28.9 mL, 0.202 mol) and anisole (9.6 mL, 25 v%) were added, and the reaction mixture was degassed by three freeze−pump−thaw cycles. After stirring for 1 h at room temperature, CuBr (0.0363 g, 0.253 mmol) was added, and the flask was placed in a preheated oil bath at 70 °C. The polymerization was stopped after 10 h by cooling to room temperature and opening the flask to air. GPC was used to analyze the molecular weight

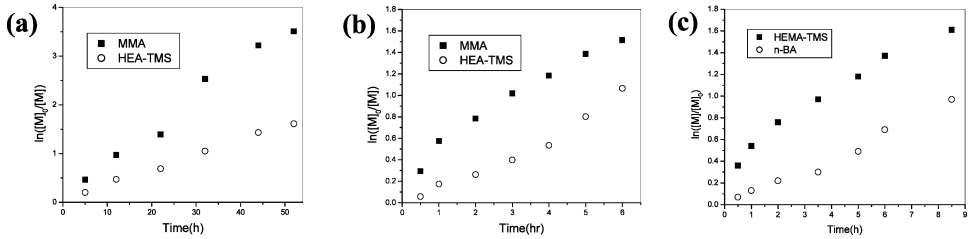


**Figure 1.** Monomer conversions in spontaneous gradient copolymerizations: (a) **I**, (b) **II**, and (c) **III**.

($M_{n,app}$) and the polydispersity. The polymer was purified by evaporating the solvent and the monomer under vacuum ($2 \times 10^{-2}$ mbar) at room temperature, dissolving the crude polymer in chloroform (150 mL), passing through a column (2 cm × 10 cm) of neutral alumina, removing the solvent by rotary evaporation, and drying under high vacuum at room temperature for 24 h. Yield: 0.7 g of isolated polymer ($DP_{sc,grav} = 10$, $DP_{sc,GC} = 12$). Monomer conversion was 2.6% of *n*-BA (GC); $M_n$ (GPC) = 157 000; $M_w/M_n = 1.20$.

p[(MMA-*grad*-(BPE-*graft*-*n*-BA)] (**IIA-2**). The reaction procedure was the same as the above reaction (**IIA-1**). Polymerization was stopped after 52 h. Yield: 2.3 g of isolated polymer ($DP_{sc,grav} = 32$, $DP_{sc,GC} = 30$). Monomer conversion was 7.5% of *n*-BA (GC); $M_n$ (GPC) = 252 000; $M_w/M_n = 1.29$.

p[(MMA-*grad*-(BPE-*graft*-*n*-BA)] (**IA-1**). The reaction procedure was the same as the above reaction (**IIA-1**). Polymerization was stopped after 50 h. Yield: 2.0 g of isolated polymer ($DP_{sc,grav} = 45$, $DP_{sc,GC} = 40$). Monomer conversion was 10% of *n*-BA (GC); $M_n$ (GPC) = 327 000; $M_w/M_n = 1.32$.

p(HEMA-TMS-*grad*-*n*-BA) (**III**): initial feed ratio (HEMA-TMS:*n*-BA = 5:1). The procedure was the same as described reaction (**I**) except that PMDETA was used as a ligand instead of dNbpy. Monomer conversion was 80% of HEMA-TMS and 62% of *n*-BA (GC); $M_n$ (GPC) = 48 000; $M_w/M_n = 1.26$.

p(BPEM-*grad*-*n*-BA) (**IIIA**). The reaction procedure was the same as the reaction (**IIA**). $^1$H NMR (300 MHz, $CDCl_3$, $\delta$ in ppm): pBPEM part: 4.52 (1H, quart, $J = 6.8$ Hz, Br−C*H*-$CH_3$); 4.36 (2H, bs, −O−$CH_2$−C$H_2$−OCO−CH−Br); 4.15 (2H, bs, −O−C$H_2$−$CH_2$−O−CO−CH−Br); 1.82 (overlapped, d, $J =$ 6.8 Hz, Br−CH−C$H_3$); 2.0−1.4 (overlapped, m, C$H_2$−C−$CH_3$); 1.2−0.9 (overlapped, bs, $CH_2$−C−C$H_3$). p-*n*-BA part: 4.05 (2H, t, −O−C$H_2$$CH_2$$CH_2$$CH_3$); 1.6 (q, 2H, −O−$CH_2$C$H_2$$CH_2$$CH_3$); 1.38 (overlapped, sixtet, 2H, −O−$CH_2$$CH_2$C$H_2$$CH_3$); 0.9 (t, 3H, −O−$CH_2$$CH_2$$CH_2$C$H_3$); 2.0−1.7 (overlapped, 2H, C$H_2$−CH); 2.5−2.1 (1H, $CH_2$−C*H*). $M_n$ (GPC) = 49 000; $M_w/M_n = 1.29$, DP = 390.

p[(MMA-*grad*-(BPE-*graft*-*n*-BA)] (**IIIA-1**). The reaction procedure was the same as the reaction (**IIA-1**). Polymerization was stopped after 48 h. Yield: 2.8 g of isolated polymer ($DP_{sc,grav} = 38$, $DP_{sc,GC} = 40$). Monomer conversion was 10% of *n*-BA (GC); $M_n$ (GPC) = 256 000; $M_w/M_n = 1.37$.

## Results and Discussion

Copolymers with different gradients of grafting densities along the backbone were prepared by ATRP according to Scheme 1. In contrast to the forced gradient technique, where the gradients along the backbone are varied by slow addition of one comonomer during the course of the polymerization, spontaneous gradients result from the difference in reactivities of the two monomers and their initial feed ratios. It is important to choose two monomers which have sufficiently large differences in reactivity ratios to ensure that one monomer propagates faster than the other. Acrylate/methacrylate pairs were chosen to prepare the gradient copolymers discussed herein because these monomers have significantly different reactivities. Two systems were used to prepare the spontaneous gradients: copolymerization of MMA with HEA-TMS and copolymerization of *n*-BA with HEMA-TMS. Both pairs consisted of an acrylate and a methacrylate using one comonomer

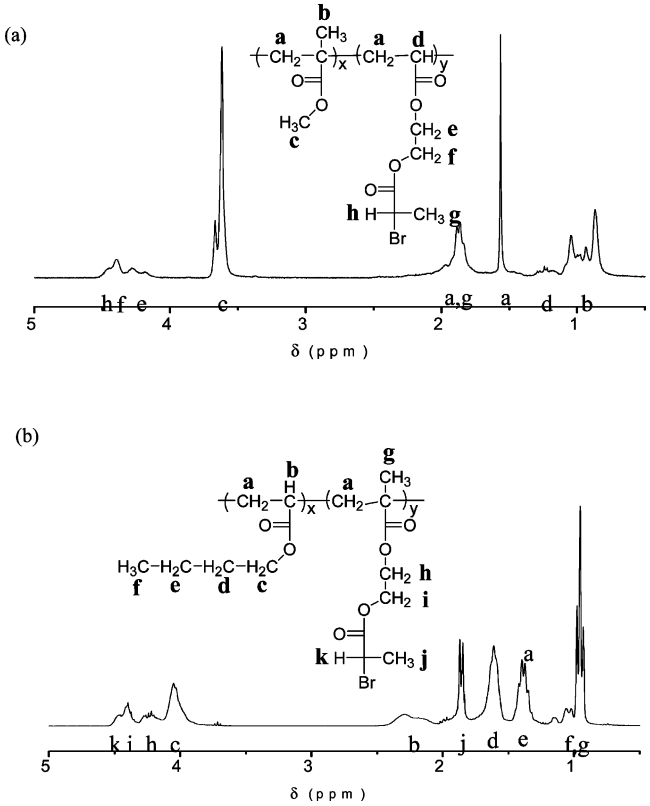


**Figure 2.** $^1$H NMR spectra of macroinitiators (a) **IIA** and (b) **IIIA**.

that could be derivatized to yield an initiating moiety for the subsequent brush synthesis.

The spontaneous gradient copolymerization (**I**) of MMA and HEA-TMS with a initial feed ratio of 1:1 was conducted with dNbpy as a ligand. The monomer was diluted by half with anisole to reduce viscosity. As shown in Figure 1a, the first-order kinetic plot showed that MMA was polymerized much faster than HEA-TMS, as expected. After 52 h the conversions of MMA and HEA-TMS were 97% and 75%, respectively. The resulting polymer had a $M_n = 7.1 \times 10^4$ g/mol and a polydispersity of $M_w/M_n = 1.2$. Another copolymerization of MMA and HEA-TMS was carried out with an initial feed ratio of 3:1. The semilogarithmic kinetic plot is linear, demonstrating that the number of the active species is constant throughout the polymerization and that the reaction is first order in each monomer concentration (Figure 1b).

The copolymerization of HEMA-TMS and *n*-BA (**III**) was carried out with a initial feed ratio of 1:5 in 50% of anisole. Polymerization was stopped after 8.5 h, at which point the conversion of HEMA-TMS and *n*-BA reached 62% and 80%, respectively (Figure 1c). In all cases monomer conversion increased monotonically with time.

**Table 1. Conditions and Results of the Gradient Copolymerizations**

| backbone[a] | catalyst | monomers ($M_1$/$M_2$) | [$M_1$]:[$M_2$]:[I]:[$Cu^+$]:[ligand] | temp (°C) | time (h) | $M_n$[b] ($\times10^{-4}$) | PDI[b] | conv$_1$ (%) | conv$_2$ (%) |
|---|---|---|---|---|---|---|---|---|---|
| **I** | CuBr/(dNbpy)$_2$ | MMA/HEA-TMS (1:1) | 300:300:1:1:2 | 85 | 52 | 7.1 | 1.28 | 97 | 75 |
| **II** | CuBr/PMDETA | MMA/HEA-TMS (3:1) | 450:150:1:1:1 | 85 | 6 | 5.1 | 1.21 | 78 | 65 |
| **III** | CuBr/PMDETA | HEMA-TMS/*n*-BA (1:5) | 100:500:1:1:1 | 85 | 8.5 | 4.8 | 1.26 | 80 | 62 |

[a] **I**: MMA/HEA-TMS (initial feed ratio: 1/1); **II**: MMA/HEA-TMS (initial feed ratio: 3/1); **III**: *n*-BA/HEMA-TMS (initial feed ratio: 5/1). [b] Calibrated with linear PMMA standards.

**Table 2. Data for Macroinitiator Synthesis**

| macroinitiator[a] | $M_n$[b] ($\times10^{-4}$) | PDI | DP[c] | fraction of initiator GC | fraction of initiator NMR | no. of initiator groups per chain[d] |
|---|---|---|---|---|---|---|
| **IA** | 7.2 | 1.32 | 515 | 43 | 45 | 232 |
| **IIA** | 5.2 | 1.20 | 450 | 22 | 20 | 90 |
| **IIIA** | 4.9 | 1.29 | 390 | 20 | 22 | 86 |

[a] **IA**: macroinitiator from copolymer **I**; **IIA**: macroinitiator from copolymer **II**; **IIIA**: macroinitiator from copolymer **III**. [b] Calibrated with linear PMMA standards. [c] Determined by conversion from GC. [d] Determined by $^1$H NMR spectroscopy.

The above three copolymers, pMMA-*grad*-HEA-TMS (**I** and **II**) and pHEMA-TMS-*grad*-*n*-BA (**III**), were transformed to the corresponding macroinitiators, pMMA-*grad*-BPE (**IA** and **IIA**) and pBPEM-*grad*-*n*-BA (**IIIA**). The transformed macroinitiators were characterized by GPC and $^1$H NMR spectroscopy. Because these macroinitiators were to function as the brush backbones, extensive characterization was needed to provide information about the initiator density and distribution along the backbone. The final copolymer compositions were determined by $^1$H NMR spectroscopy after functionalization to the corresponding macroinitiators (Figure 2). For copolymer backbones **I** and **II**, the integration area of $-OCH_3$ at 3.6 ppm from MMA and five protons from BPE (1H, Br$-CH-CH_3$ at 4.52 ppm, 2H, $-O-CH_2-CH_2-OCO-CH-Br$ at 4.36 ppm, and 2H, $-O-CH_2-CH_2-O-CO-CH-Br$ at 4.15 ppm) were compared to get the final copolymer compositions (Table 2).

For macroinitiator **IIA**, the calculations based on integration area revealed that the ratio between MMA and BPE was 80:20 (Figure 2a). The actual number of initiating groups along the backbone was calculated from the total DP of the backbone obtained from the final conversion of each monomer determined by GC and the mole fraction of BPE units in the backbone determined by $^1$H NMR spectroscopy. Thus, macroinitiator **IIA** contained 90 units (20% out of total DP = 450) of the initiating groups.

For macroinitiator **IIIA**, the integration area of $-CH_2-$ next to ester group from *n*-BA at 4.00 ppm and five protons from BPEM were compared to calculate the composition. The ratio between BPEM and *n*-BA was calculated from these integration areas to be 78:22. Therefore, for the macroinitiator **IIIA**, an average of 86 units (22% out of total DP = 390) of the initiator are contained in the backbone. The results for all macroinitiators are listed in Table 2.

The grafted copolymer brushes were synthesized by grafting *n*-BA from p(MMA-*grad*-BPE) and p(BPEM-*grad*-*n*-BA) macroinitiators. Figure 3 shows the GPC traces of the starting material (**I**, p(MMA-*grad*-HEA-TMS)), the macroinitiator (**IA**, p(MMA-*grad*-BPE)), and two of the corresponding brush copolymers with different DP of the side chains (**IA-1**, **IIA-2**). All of the brush polymerizations were carried out with 10 vol % anisole as a solvent, and the [BA]:[BPEM] ratio remained constant at 400:1. $CuBr_2$ was added initially to reduce the amount of spontaneously generated radical termination due to the persistent radical effect.[27]

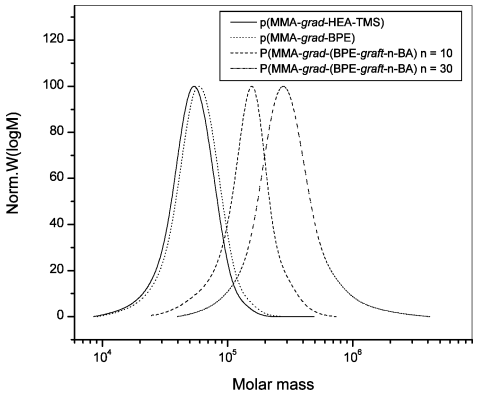


**Figure 3.** GPC traces of (a) the gradient copolymer backbone **II**, (b) the macroinitiator **IIA** after transformation from **I**, and (c) the resulting brushes **IIA-1** and **IIA-2** from macroinitiator **IIA**.

As shown in Figure 3, there was a slight shift of the GPC traces from the starting copolymer to the resulting macroinitiator. During the synthesis of the brushes, the traces were shifted completely, indicating high molecular weight brushes were formed. There was no significant tailing or shoulders, indicating negligible contribution of side reactions such as intermolecular brush−brush coupling. The brush syntheses appeared to proceed in a controlled fashion since the polydispersities for all cases remained similar to the backbone copolymers (Table 3).

**Calculation of Instantaneous Composition along the Backbone.** At several times during the backbone synthesis, aliquots were taken to measure the percent conversion of each comonomer. From these conversion data, the instantaneous fraction of HEA-TMS and HEMA-TMS, to be transformed to BPE and BPEM, respectively, could be calculated. Figure 4 displays the instantaneous fraction of TMS groups for each copolymer backbone with respect to the degree of polymerization along the chain. The first plot shows a progressive gradient in the copolymer composition for **I**. The results indicate this copolymer is ~35% HEA-TMS at one end and increases to nearly 80% at the other end. Instantaneous composition (% IC) of HEA-TMS along copolymer **I** was calculated from the monomer conversion using the equation % $IC_{HEA-TMS} = \Delta_{HEA-TMS}/(\Delta_{HEA-TMS} + \Delta_{MMA})$, where $\Delta$ is the change in the percent conversion of monomers since the previous measurement. Because each instantaneous composition is the cumulative composition since the previous measurement, the average value of DP was taken between two measurement points obtained from conversion. Approximately 5% HEA-TMS at one end and nearly 55% at the other end were calculated for the gradient copolymer **II**, for which the initial feed ratio was 3:1 (MMA to HEA-TMS). In this case $\Delta_{MMA}$ should be

**Table 3. Conditions and Results of the Gradient Brushes from the Macroinitiators**

| brushes[a] | catalyst system | macroinitiator | [M]:[I]:[$Cu^+$]:[$Cu^{2+}$]:[ligand] | temp (°C) | time (h) | $M_n$[b] ($\times 10^{-5}$) | PDI | DP GC[c] | DP GRAV[d] |
|---|---|---|---|---|---|---|---|---|---|
| **IA-1** | CuBr/(dNbpy)$_2$ | **IA** | 400:1:0.5:0.005:1 | 70 | 50 | 3.27 | 1.32 | 40 | 45 |
| **IIA-1** | CuBr/(dNbpy)$_2$ | **IIA** | 400:1:0.5:0.005:1 | 70 | 24 | 1.57 | 1.20 | 12 | 10 |
| **IIA-2** | CuBr/(dNbpy)$_2$ | **IIA** | 400:1:0.5:0.005:1 | 70 | 52 | 2.52 | 1.29 | 30 | 32 |
| **IIIA-1** | CuBr/(dNbpy)$_2$ | **IIIA** | 400:1:0.5:0.005:1 | 70 | 48 | 2.56 | 1.37 | 40 | 38 |

[a] **IA-1**: brush from macroinitiator **IA**; **IIA-1**: brush from macroinitiator **IIA**; DP of the side chains = 10; **IIA-2**: brush from macroinitiator **IIA**; DP of the side chains = 30; **IIIA-1**: brush from macroinitiator **IIIA**. [b] GPC calibrated with linear PMMA standards. [c] Calculated from conversion determined by GC. [d] Calculated from conversion determined by gravimetry.

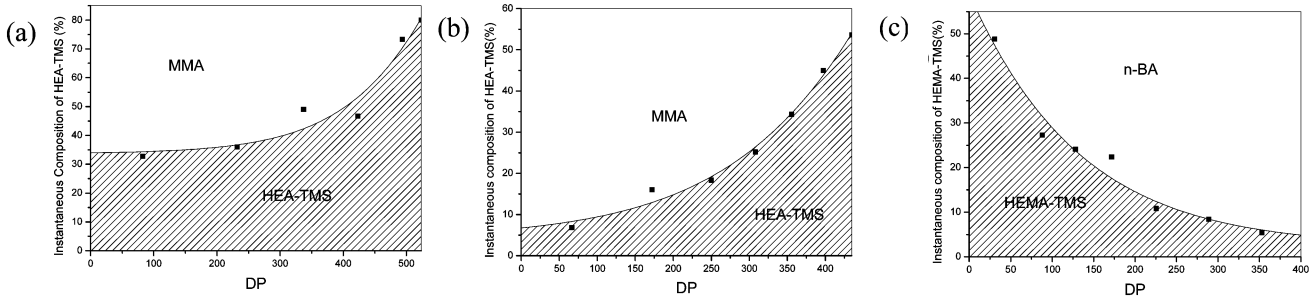


**Figure 4.** Instantaneous composition of the gradient copolymers (a) **I**, (b) **II**, and (c) **III**.

**Table 4. Conversion Data Used for the Calculation of the Reactivity Ratios**

| $M_1$ | $M_2$ | $[M_1]_0$:$[M_2]_0$[a] | $conv_1$ (%)[b] | $conv_2$ (%)[b] |
|---|---|---|---|---|
| MMA | HEA-TMS | 3:1 | 43.7/54.3/63.9/69.4 | 16/23.1/32.8/41.4 |
| MMA | HEA-TMS | 5:1 | 36.9/50.5/63.3/70 | 12.4/21.6/33/40.8 |
| HEMA-TMS | *n*-BA | 1:3 | 38.4/50.6/67.5/75.5 | 9.2/15/36.2/52.6 |
| HEMA-TMS | *n*-BA | 1:5 | 30/41.8/53.1/62.2/69.3 | 6.3/12.6/19.7/26/38.7 |

[a] Initial feed ratio. [b] Five conversion data points from the aliquots taken throughout the polymerization.

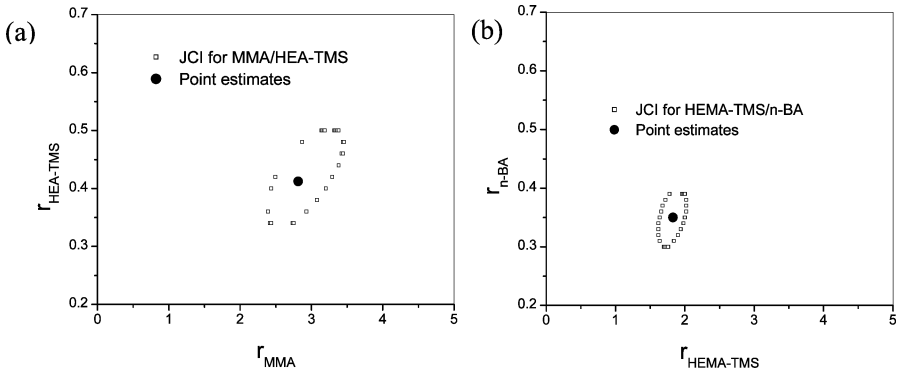


**Figure 5.** 95% joint confidence intervals and point estimates for the copolymerization of (a) MMA/HEA-TMS and (b) HEMA-TMS/*n*-BA.

tripled in the denominator to give the equation % $IC_{HEA-TMS} = \Delta_{HEA-TMS}/(\Delta_{HEA-TMS} + 3\Delta_{MMA})$. Note that the different range of the instantaneous compositions can be accomplished by the different initial feed ratios. For p(HEMA-TMS-*grad*-*n*-BA) (**III**), which was the precursor of pBPEM-*grad*-*n*-BA, HEMA-TMS was incorporated into the backbone faster than *n*-BA. Therefore, the instantaneous composition with ~55% HEMA-TMS at the beginning decreased to around 10% at the chain end. The instantaneous composition of HEMA-TMS along the backbone of copolymer **III** with the initial feed ratio of 1:5 from HEMA-TMS to *n*-BA was calculated from the equation % $IC_{HEMA-TMS} = \Delta_{HEMA-TMS}/(5\Delta_{HEMA-TMS} + \Delta_{n-BA})$.

**Calculations of Reactivity Ratios.** To estimate reactivity ratios for both pairs of monomers (MMA/HEA-TMS and HEMA-TMS/n-BA), nonlinear least-squares calculations were used. The equations used for nonlinear least-squares calculations were explicitly provided in our previous publication.[10] A conversion range of 20−50% should be covered when using an integrated form of the composition equation because low conversion copolymer composition values calculated from residual feed analysis can have large errors and may be biased by preferential initiation of one monomer by the initiating radical. The "sum-of-squares space" (SS-space) approach was used to calculate joint confidence intervals (JCIs).[10]

To calculate the monomer reactivity ratios and 95% JCIs for the copolymerizations, the same catalyst system should be applied. Moreover, two sets of monomer conversion data with at least three data points which can be obtained from the copolymerization with different monomer feed ratios were included.

Table 4 shows the monomer conversion data that were used for the calculations. One more copolymerization was carried out for each monomer pairs with different initial feed ratios. Among several data points from the reaction, four conversion data, which belonged to roughly 20−50% conversion range, were selected to optimally

**Scheme 2. Theoretical Behavior of Gradient Brushes upon Adsorption onto Mica**[a]

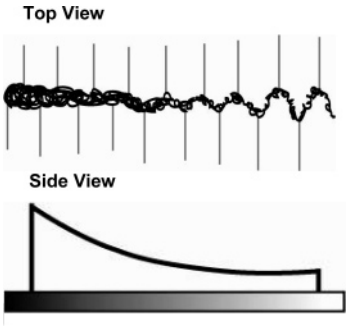


[a] As viewed from to the top, there should be a region of fairly extended backbone indicative of the densely grafted head that gradually becomes more flexible as more spacers are incorporated (tail region). Looking at the molecule from the side, gradient brushes should exhibit a sloping profile, a consequence of the change in grafting density resulting in less side chains desorbing from the surface. However, the slopes exhibited by the gradient brushes depend largely on the monomer composition change along the backbone, i.e., instantaneous composition of backbone as polymerization proceeds. Note that adsorbed side chain density will be constant for all samples. Side view slope is exaggerated for emphasis.

estimate the reactivity ratios. The joint confidence intervals (JCI) and point estimates for the two different series of monomer systems are shown in Figure 5. The point estimate for the MMA/HEA-TMS system is slightly different from that of the HEMA-TMS/*n*-BA system. The reactivity ratios in the MMA/HEA-TMS system are $r_{MMA} = 2.8$ and $r_{HEA-TMS} = 0.41$. For the HEMA-TMS + *n*-BA system, $r_{HEMA-TMS} = 1.9$ and $r_{MMA} = 0.35$.

**AFM Analysis.** Visual conformation of various gradient p-*n*-BA brush molecules was undertaken using tapping mode atomic force microscopy (TMAFM). Samples were prepared by spin-casting dilute chloroform solutions of each sample onto mica.

**Theoretical Behavior of Gradient Brushes upon Adsorption onto Mica.** Scheme 2 shows the conformation adopted by the gradient brushlike macromolecules on a surface. The variation in grafting density along the backbone results in the coexistence of different morphologies in a single molecule. Above a certain grafting density, not all of the side chains present can adsorb onto the surface due to space constraints. Thus, a large fraction of the side chains segregate along the backbone above the substrate surface, creating a bulky head region as seen in Scheme 2. In this region, the repulsive interactions between the adsorbed side chains will cause the backbone extension. However, when one goes below a certain grafting density, there is enough room on the surface to accommodate all side chains, creating the flat and less distinct tail region. In addition, the reduced repulsion between adsorbed side chains results in the contraction of the backbone.

On the basis of the information from the instantaneous composition plot, the profile of **IA-1** should contain a distinct head region that will gradually decrease in height along the backbone until it reaches a plateau, i.e., a tail region. On the other hand, the molecules of **IIA-2** and **IIIA-1** will have different profiles from **IA-1** because of the change in grafting density and instantaneous composition. Because of the decrease in side chain density, both brushes should contain shorter regions of relatively stretched backbone, i.e., small head region, and a greater portion of the more flexible spacer regions, i.e., less side chain repulsion causing greater contraction. Even though the grafting densities are the same, **IIIA-1** is expected to be more flexible than **IIA-2** because the backbone of **IIIA-1** is composed of soft *n*-BA spacer monomers.

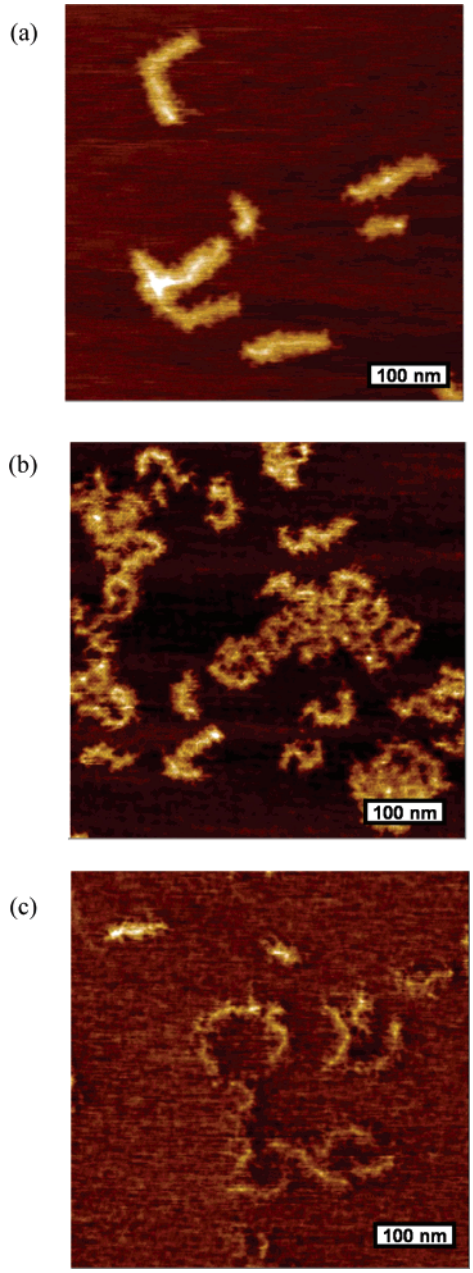


**Figure 6.** AFM images of the gradient brushes. (a) Height image for **IA-1** from TMAFM. The gradient is clearly visible along the backbone, a distinctive "head" region corresponding to higher grafting density and a "tail" of loosely grafted p-*n*-BA side chains (500 nm × 500 nm). (b) Height image for **IIA-2** from TMAFM. For **IIA-2**, the gradient is difficult to see even though the intrinsic flexibility of the backbone is clearly observed; i.e., there is distinct curvature present due to its lower grafting density compared to that of **IA-1** (500 nm × 500 nm). (c) Height image for **IIIA-1** from TMAFM. Similar to **IIA-2**, the gradient is difficult to see, but there is an observable curvature to the molecules (500 nm × 500 nm).

From TMAFM experiments, single molecules of each sample were observed, confirming their brushlike architecture. Parts a−c of Figure 6 are micrographs of the three brushes, **IA-1**, **IIA-2**, and **IIIA-1**, respectively. The gradient is clearly visible in **IA-1**, which incorporated a higher fraction of initiating groups into the backbone.

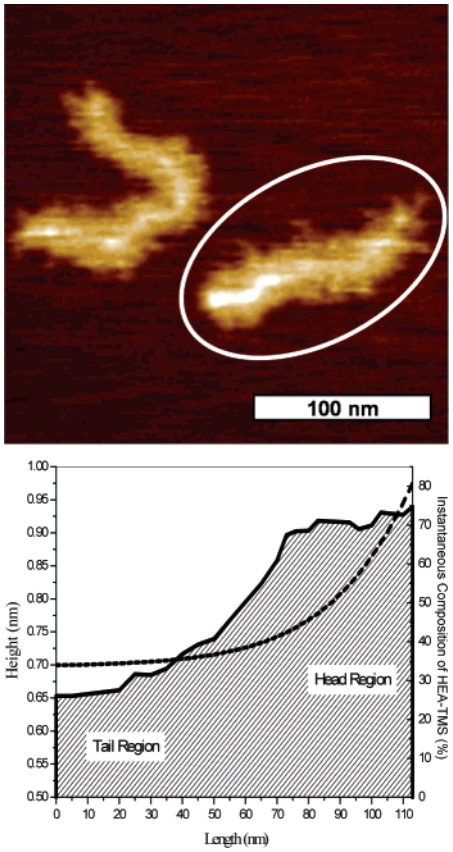


**Figure 7.** Height profile of a typical **IA-1** molecule. The gradient characteristic of **IA-1** is clearly visible from the extracted height profile. The source of the asymmetry along the backbone is change in amount of desorbed side chains corresponding to the change in grafting density, i.e., fraction of initiating groups incorporated into the macroinitiator determined from the instantaneous composition curve (dashed line) (250 nm × 250 nm).

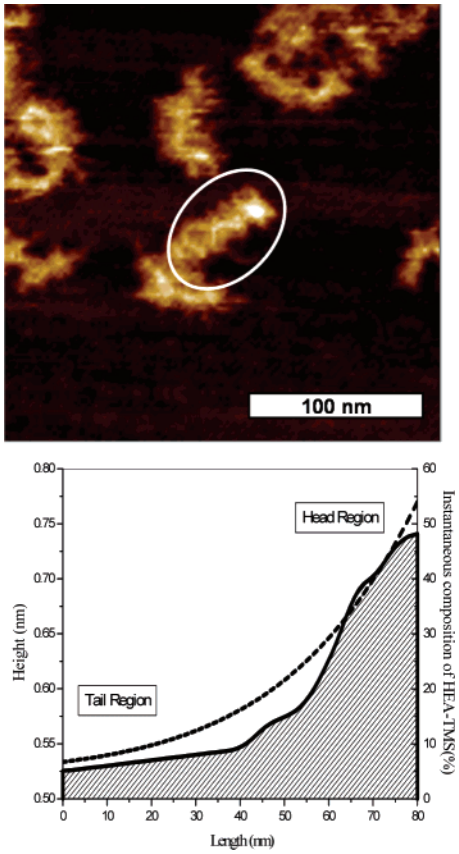


**Figure 8.** Height profile of a typical **IIA-2** molecule. Even though the gradient nature of this sample is difficult to see overall, there are single brushes present that do exhibit theoretically predicted behavior. For instance, the encircled brush has a distinct peak that corresponds to the densely grafted region of the molecule that quickly diminishes in brightness. The abrupt and dramatic decrease in height corresponds to the change in copolymer composition as copolymerization proceeded to completion similar to what is observed in the instantaneous composition plot (dashed line).

This difference in copolymer composition along the **IA-1** backbone is evidenced by the presence of a brighter "head", which is the densely grafted portion, and a less distinct tail containing fewer grafted side chains, behaving as theoretically predicted. On the other hand, confirmation of the gradients for **IIA-2** and **IIIA-1** is impeded by the lower grafting densities along the macroinitiators of these samples. With a loosely grafted system, analysis and visualization by AFM become a challenge due to decreased contrast between the side chains and the backbone. An added complication comes from decreased side chain repulsion, which results in increased backbone contraction upon adsorption onto the substrate. The combination of these two events makes it difficult to fully appreciate the uniqueness of these samples since the micrographs show relatively uniform profiles along the backbone for these latter two samples, a stark contrast to the sloping profile exhibited by **IA-1**.

Height profiles for typical molecules of each sample were extracted. In the case of densely grafted bottle brushes without a gradient of initiating group, the amount of absorbed side chains and desorbed side chains will be fairly constant along the backbone. But for gradient brushes, densely grafted head regions will have extra desorbed side chains compared to losely grafted tail regions, a reflection of compositional change along the backbone. As a result, the gradient nature of these brushes is manifested by height differences between head and tail regions which are comparable to the instantaneous composition profiles during synthesis of backbone. As predicted from above, the height profile of **IA-1** follows a sloping trend similar to the instantaneous composition curve (Figure 7). Similarly, the abrupt change in heights in **IIA-2** profile reflects the copolymerization of MMA and HEA-TMS as observed from its instantaneous composition plot (Figure 8). And finally, the extracted profile of **IIIA-1** also follows the trend of the instantaneous plot obtained wherein the gradient nature of the molecule is barely detectable because there are very few initiating groups along the copolymer backbone and small amount of desorbed side chains (Figure 9).

In addition to visualization, statistical analysis of lengths was performed for each p*n*BA gradient brush. Results are summarized in Table 5. The polydispersity index calculated from length analysis correlates well with GPC results. As expected, contour length results for all three samples reflect the flexibility of the backbones, with length per monomeric unit values less than the C−C−C section length of 0.25 nm. Since the calculated values are within statistical error of each other, it is difficult to obtain a linear correlation between gradient density and molecular lengths though there is a definite decrease from **IA-1** to **IIA-2** and **IIIA-1**. Ironically, it is the increased gradient nature of the

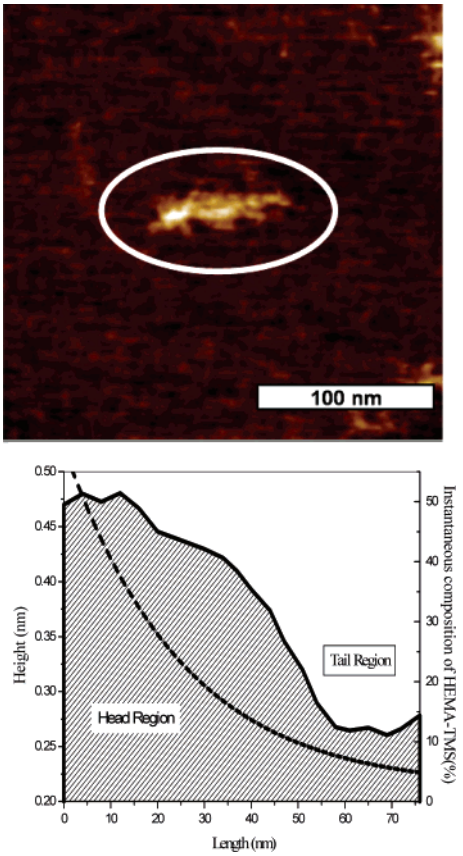


**Figure 9.** Height profile of a typical **IIIA-1** molecule. Similar to **IIA-2**, the gradient nature of this molecule is barely detectable because there are very few initiating groups along the copolymer backbone, but the height profile does exhibit the same trend as that of for the instantaneous composition (dashed line). Grafting longer *n*-BA side chains to increase contrast between the different regions of the molecule may aid in future AFM experiments involving weak gradient brush molecules (250 nm × 250 nm).

**Table 5. Length Profile Summary**

| sample | $L_n$[a] (nm) | $D$[b] (nm) | corrected $L_n$[c] (nm) | $l_m$ (nm)[d] | PDI[e] |
|---|---|---|---|---|---|
| **IA-1** | 104 ± 4 | 14 ± 3 | 90 ± 7 | 0.175 ± 0.02 | 1.27 ± 0.03 |
| **IIA-2** | 89 ± 2 | 14 ± 1 | 75 ± 2 | 0.167 ± 0.02 | 1.27 ± 0.02 |
| **IIIA-1** | 79 ± 3 | 15 ± 1 | 64 ± 3 | 0.164 ± 0.02 | 1.24 ± 0.03 |

[a] Number-average backbone length including side chain protrusion. [b] Average width of molecules, i.e., two side chain lengths, needed to correct for overestimation of contour length due to presence of side chains at ends. [c] Number-average backbone length corrected for side chains protrusion at ends of molecule. [d] Length per monomeric unit of backbone, corrected $L_n$/DP of the backbone. [e] Polydispersity index = $L_w/L_n$.

latter two samples that is to blame for the difficulty in their analysis and characterization.

Thus, atomic force microscopy is an extremely powerful and versatile technique that enables one to directly visualize molecular shape and architecture as well as to quantitatively determine molecular dimensions, making it an essential tool in polymer science.

## Conclusions

ATRP was used to prepare well-defined, spontaneous gradient copolymers of MMA/HEA-TMS and *n*-BA/HEMA-TMS. The instantaneous compositions of the TMS-containing monomer with respect to DP of the copolymer demonstrated that there was a gradient in copolymer composition along the backbone. Various ranges of gradient compositions were accomplished by using different initial feed ratios. The resulting gradient copolymers were transformed to the corresponding macroinitiators, p(MMA-*grad*-BPE) and p(BPEM-*grad*-*n*-BA). These macroinitiators were subsequently employed to prepare high molecular weight and low polydispersity molecular brushes with gradients of grafting density along the backbone. The gradient shape of the brushes was verified by AFM.

**Acknowledgment.** This work was financially supported by the National Science Foundation (ECS 01-03307, CHE 00-90409). The authors also thank Dr. Brent Sumerlin for helpful discussions.

## References and Notes

(1) Sheiko, S. S.; Moller, M. *Chem. Rev.* **2001**, *101*, 4099−4123.
(2) Schappacher, M.; Deffieux, A. *Macromolecules* **2000**, *33*, 7371−7377.
(3) Tsukahara, Y.; Tsutsumi, K.; Yamashita, Y.; Shimada, S. *Macromolecules* **1990**, *23*, 5201−5208.
(4) Dziezok, P.; Sheiko, S. S.; Fischer, K.; Schmidt, M.; Moller, M. *Angew. Chem., Int. Ed. Engl.* **1997**, *36*, 2812−2815.
(5) Boerner, H. G.; Duran, D.; Matyjaszewski, K.; da Silva, M.; Sheiko, S. S. *Macromolecules* **2002**, *35*, 3387−3394.
(6) Matyjaszewski, K.; Ziegler, M. J.; Arehart, S. V.; Greszta, D.; Pakula, T. *J. Phys. Org. Chem.* **2000**, *13*, 775−786.
(7) Pakula, T. *Macromol. Theory Simul.* **1996**, *5*, 987−1006.
(8) Greszta, D.; Matyjaszewski, K.; Pakula, T. *Polym. Prepr. (Am. Chem. Soc., Div. Polym. Chem.)* **1997**, *38*, 709−710.
(9) Arehart, S. V.; Matyjaszewski, K. *Polym. Prepr. (Am. Chem. Soc., Div. Polym. Chem.)* **1999**, *40*, 458−459.
(10) Arehart, S. V.; Matyjaszewski, K. *Macromolecules* **1999**, *32*, 2221−2231.
(11) Ziegler, M. J.; Matyjaszewski, K. *Macromolecules* **2001**, *34*, 415−424.
(12) Sheiko, S. S.; Prokhorova, S. A.; Beers, K. L.; Matyjaszewski, K.; Potemkin, I. I.; Khokhlov, A. R.; Moeller, M. *Macromolecules* **2001**, *34*, 8354−8360.
(13) Lord, S. J.; Sheiko, S. S.; LaRue, I.; Lee, H.-I.; Matyjaszewski, K. *Macromolecules* **2004**, *37*, 4235−4240.
(14) Subbotin, A.; Saariaho, M.; Ikkala, O.; ten Brinke, G. *Macromolecules* **2000**, *33*, 3447.
(15) Fredrickson, G. H. *Macromolecules* **1993**, *26*, 2825−2831.
(16) Wintermantel, M.; Gerle, M.; Fischer, K.; Schmidt, M.; Wataoka, I.; Urakawa, H.; Kajiwara, K.; Tsukahara, Y. *Macromolecules* **1996**, *29*, 978−983.
(17) Yamada, K.; Miyazaki, M.; Ohno, K.; Fukuda, T.; Minoda, M. *Macromolecules* **1999**, *32*, 290−293.
(18) Neugebauer, D.; Zhang, Y.; Pakula, T.; Sheiko, S. S.; Matyjaszewski, K. *Macromolecules* **2003**, *36*, 6746−6755.
(19) Beers, K. L.; Gaynor, S. G.; Matyjaszewski, K.; Sheiko, S. S.; Moeller, M. *Macromolecules* **1998**, *31*, 9413−9415.
(20) Boerner, H. G.; Beers, K.; Matyjaszewski, K.; Sheiko, S. S.; Moeller, M. *Macromolecules* **2001**, *34*, 4375−4383.
(21) Neugebauer, D.; Sumerlin, B. S.; Matyjaszewski, K.; Goodhart, B.; Sheiko, S. S. *Polymer* **2004**, *45*, 8173−8179.
(22) Sumerlin, B. S.; Neugebauer, D.; Matyjaszewski, K. *Macromolecules* **2005**, *38*, 702−708.
(23) Pyun, J.; Matyjaszewski, K. *Chem. Mater.* **2001**, *13*, 3436−3448.
(24) Neugebauer, D.; Zhang, Y.; Pakula, T.; Matyjaszewski, K. *Polymer* **2003**, *44*, 6863−6871.
(25) Beers, K. L.; Boo, S.; Gaynor, S. G.; Matyjaszewski, K. *Macromolecules* **1999**, *32*, 5772−5776.
(26) Matyjaszewski, K.; Patten, T. E.; Xia, J. H. *J. Am. Chem. Soc.* **1997**, *119*, 674−680.
(27) Goto, A.; Fukuda, T. *Prog. Polym. Sci.* **2004**, *29*, 329−385.

MA051231Z